

Absorption Spectroscopic Studies of Chip-scale Rubidium Atomic Vapour Cells in a Compact 3D Printed Magneto-Optic Package

M S Giridhar*, S P Karanth, Akshaya, S Elumalai & K V Sriram

Laboratory for Electro-Optics Systems, Indian Space Research Organization, Bengaluru 560 094, India

Received 16 February 2023; accepted 28 March 2023

This paper describes the design, development and spectroscopic studies of chip-scale Rb atomic vapour cell developed in the authors' laboratory. A compact magneto-optic package for the chip-scale Rb cell comprising of TEC integrated VCSEL source, silicon p-i-n photo detector and a hemispherical lens for light collimation is reported. The package is manufactured using commercial 3D printing technology. A PC based data acquisition system has been developed to provide real time analysis of the captured spectral data of the Rb chip by laser interrogation of the D1 hyperfine transition. Doppler broadened absorption resonance lines of technological importance have been recorded for transitions $^{85}\text{Rb}(^2\text{S}_{1/2} F=2 \rightarrow ^2\text{P}_{1/2} F'=2,3)$ having absorption amplitude 1.24 V and FWHM 850 MHz and $^{87}\text{Rb}(^2\text{S}_{1/2} F=1 \rightarrow ^2\text{P}_{1/2} F'=1,2)$ has absorption amplitude 0.47 V and FWHM 567 MHz at cell temperature of 70 °C. Further, the chip-scale Rb atomic cell in the magneto-optical package will be explored to develop atomic sensors for space applications.

Keywords: Chip-scale vapour cell; Absorption spectroscopy; 3D printing; Tunable diode laser spectroscopy

1 Introduction

Rapid advances are being made in the area of miniature quantum sensors based on hot atomic vapours. In recent times, groups around the world have demonstrated compact quantum devices such as magnetometers^{1,2}, gyroscopes³, frequency stabilized lasers^{4,5}, frequency standards^{6,7}, atomic receivers⁸ and THz detectors⁹. An important building block in all these systems is the chip-scale alkali metal vapour cell¹⁰. This micro-machined component holds the alkali vapour such as Rubidium (Rb) or Cesium whose atoms are optically interrogated to obtain absorption spectra. In certain applications inert buffer gasses and spin polarizable atomic species such as Xe are also introduced to the vapour cell along with the alkali metal. Various configurations of chip-scale cells such as planar^{11,12}, spherical¹³ cubical shapes have been developed using MEMS fabrication technologies. In this paper, we report the development of a compact magneto optic (MO) head incorporating the chip-scale Rb vapour cell manufactured in the authors' laboratory¹⁴ using deep reactive ion etching process and anodic bonding technology. The package is built using 3D printing. It comprises of self-aligning compartments for the vapour cell, Thermo Electric Cooler (TEC) integrated Vertical Cavity Surface

Emitting Laser (VCSEL) source, p-i-n photodetector and collimating lens. In addition, provisions have been made for the inclusion of annular permanent magnets, polarizing elements such as quarter wave plate, neutral density filters as required in some of the atomic sensor applications of this design of the MO package. The development this MO package is a precursor of miniature quantum sensors envisaged above. The details of the design of the MO package, heater integrated chip-scale Rb vapour cells and experimental characterisation by absorption spectroscopy are described in the following sections.

2 Design of the Magneto-optic Package

The primary design consideration of the miniature MO package was to ensure compactness and error free alignment of the constitutive components. The MO package is comprises of two parts i) the slotted housing, containing heater integrated chip-scale vapour cell optical elements, magnets and thermistor. ii) outer housing is mounted with the TEC integrated VCSEL, p-i-n detector, collimating lens and miniature connectors. The slotted housing itself comprises of two parts, one serving as holder for the components and other as a cap. The holder part of the housing has precisely machined slots into which various optical components can be inserted. Once the optical components and chip-scale cell are inserted into the

*Corresponding author: (E-mail: giri@leos.gov.in)

respective slots, a cap with corresponding slots is press-fitted on the holder to hold the components tightly in their positions and sealed with epoxy Epotech 2216. This makes the MO package immune to vibrations encountered in handling and testing of the unit. The second part is the outer housing, which holds the VCSEL laser and collimating lens and also contains a miniature electrical connector for the electrical connections from the photodiode and cell heating elements. The relatively low thermal conductivity of the polylactic acid (PLA) material of the MO package ensures good thermal isolation for the chip-scale cell. This reduces the steady state power consumption of the package. A schematic of the cross-sectional view of the MO package in its assembled form is shown in Fig. 1. Details of each component of the MO package are described in the following subsections.

2.1 Chip-scale Rb Vapour Cells

Chip-scale Rb vapour cell was fabricated using bulk silicon micromachining techniques and silicon-glass anodic bonding. The Rb vapour is produced by use of a commercial Rb dispenser pill from SAES Getters (RB/AMAX/PILL/1-0.6). The pill is inserted into a cavity of the cell during the fabrication process and thermally activated using a laser beam after it is fully encapsulated in the chip-scale cell. The cell is made up of a glass-silicon-glass stack where each substrate is 500 μm thick. Details of cell fabrication are explained in reference 14. The chip-scale vapour cell used in this work has an optical cavity 3 mm in diameter and an optical path length of 0.5 mm. This results in vapour volume of 3.5 μl . The cells are coated with indium tin oxide (ITO) films which serve as integrated heaters. The dimensions of chip-scale vapour cell are 12 mm \times 8 mm \times 1.5 mm. The boiling point of Rb is 39.48 $^{\circ}\text{C}$. At room temperature Rb metal in the chip-scale cell is in liquid phase in the form of condensed droplets on the windows of the cell. To observe atomic absorption

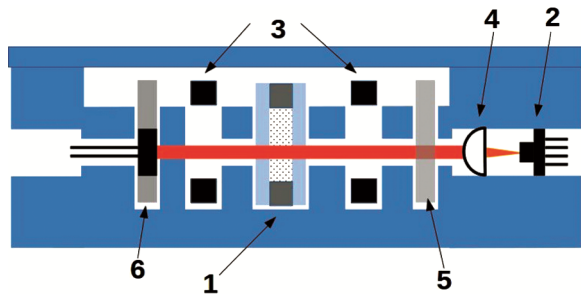


Fig. 1 — The schematic cross-section of the MO package. 1-chip-scale vapour cell, 2-VCSEL laser, 3-annular magnets, 4-collimating lens, 5-ND filter, 6- photodiode.

resonances, Rb atoms must be in vapour phase. In order to have sufficient number density of Rb atoms in vapour phase the chip-scale vapour cell has to be maintained at about 70 $^{\circ}\text{C}$. At this temperature, strong absorption resonances were observed. In this work we have developed thin film deposition recipes to directly deposit thin film heaters on the chip-scale vapour cells after laser activation of the dispenser pills. Two approaches for integrated thin film heaters were demonstrated. Nichrome (NiCr) and Indium Tin Oxide (ITO) have been used. In the first method ITO was sputter coated on the chip-scale cells in a blanket deposition process. In this process 2000 \AA of ITO was sputtered using 200 W of RF power. Both sides of the vapour cell were coated under identical conditions in subsequent runs. The transmission of the ITO films was found to be greater than 88% at 795 nm using a UV-VIS spectrophotometer (Cary UV-VIS). After the ITO coating, vacuum compatible Kapton tape was used to mask out the center portion of the cell exposing the edges for about 1 mm. Electrical contact pads are provided on either side of the chip by sputter deposition of 2000 \AA Al at 100 W DC power. Conductive epoxy H20E was manually applied to the aluminium contact pads and 25 SWG wires were attached the cell for powering the heater. In the second method, bifilar patterned NiCr heating elements were deposited on the vapour cells. The heater pattern was cut on a 500 μm thick stainless steel sheet using a wire cutting system. The vapour cell was placed in a fixture and the shadow mask was aligned with the vapour cell and loaded for NiCr deposition in an ion beam deposition system. NiCr film of 2500 \AA was deposited. ITO heaters showed a resistance of about 20 Ω and the NiCr heaters presented 600 Ω . To test the heaters, dummy vapour cells of both types, after wire attachment, were mounted on glass slides for temperature measurements using an thermal imaging camera (Jenoptik Varioscanner). The samples were placed in front of the camera at a distance of 50 cm and focus adjusted such that cell covers about 80% of the image area. The cells were supplied heater power using external power supply. With 4.0 V and 250 mA of DC current, it was observed that ITO coated cells reached a steady state temperature of 56 $^{\circ}\text{C}$. The NiCr patterned heaters attained a steady state temperature of 60 $^{\circ}\text{C}$ with a voltage of 25 V and current of about 40 mA. In the enclosed condition, it was found that under these conditions cell temperature reached around 70 $^{\circ}\text{C}$. This temperature is sufficient to the produce the required number density of Rb vapour in the cell for absorption

studies. Photographs of the two types of cells and the typical thermal camera image are given in Fig. 2.

2.2 VCSEL Source and Drive

A compact laser source with single mode output and narrow spectral line width is required for the spectroscopic interrogation of the atomic vapour in the chip-scale cell. A VCSEL source with built-in thermoelectric heater and thermistor was used in this study. The laser diode is packaged in T0-46 package (ULM794-01-TN6S46-FTT). The temperature tuning co-efficient was $0.06 \text{ nm}/^\circ\text{C}$ and current tuning co-efficient was $0.6 \text{ nm}/\text{mA}$. The spectral line width of the output is specified to be 15 MHz. A fused silica hemispherical ball lens of 10 mm diameter is positioned in front of the VCSEL diode to focus the divergent beam on to the vapour cell. Before using the laser, the dependence of center frequency on temperature was checked with a compact fiber input spectrometer (Avantes, Avspec-Mini-NIR). The resolution of the spectrometer was insufficient to determine the spectral bandwidth of the laser output, but the shift in center frequency with temperature could be clearly seen. The internal TEC was driven using a precision TEC driver from Wavelength electronics WTC3243 mounted on its evaluation board WTC3293. A $10 \text{ K}\Omega$ at 25°C NTC thermistor inside the VCSEL package was used for sensing the package temperature and used for closed loop control. A single board computer based system was developed to continuously monitor the VCSEL temperature and to compare with the set point. With this system, VCSEL temperature could be maintained with a precision of 100 mK to the set value in the range of $50 - 55^\circ\text{C}$. The VCSEL current is supplied by a Kiethley Precision source (6220). The current source is used to produce a current ramp starting from 1.45 mA to 1.55 mA in steps of 70 nA with a dwell time of 1 ms.

2.3 Photo Detector and Amplifier

Laser light, after interrogating the chip-scale vapour cell was detected by a commercial silicon p-i-n detector (BPW-34). The BPW-34 is suitable for the wavelength range 400 nm to 1100 nm and its spectral sensitivity peaks in the range 750 nm to 950 nm. The detector has a wide operating temperature (-40°C to 100°C) making it suitable for use in close proximity with the heated chip-scale cell. The output of the photodiode is given to a trans impedance amplifier based on operational amplifier AD8630. The amplifier is configured for a gain of 100 K and band width of 15 Hz by using 100 nf and $100 \text{ K}\Omega$ in its feedback path. In this mode the circuit acts as a current (I) to voltage (V) converter. The bandwidth of 15 Hz was chosen after systematic trials. It was found that with 15 Hz band width, high frequency noise pickup was effectively suppressed and at the same time, clear spectral features of Rb D1 absorption spectrum were recorded in the oscilloscope output.

3 Assembly and Testing of MO Package

As mentioned previously, the MO package comprises of two parts. i) The slotted holder, which holds the chip-scale vapour cell, magnets, filter, photodiode and thermistor. ii) the external housing with the VCSEL laser and collimating lens. The electrical connectors are also mounted on the external housing. The assembly of the MO package was carried out as follows. The laser and hemispherical lens are placed in their respective slots and potted with epoxy 2216 to arrest their positions. The electrical leads of the laser package are terminated with berg pin sockets. The chip-scale vapour cell, magnets, ND filter and photodetector assembly are all inserted in their respective slots in the slotted holder and assembled

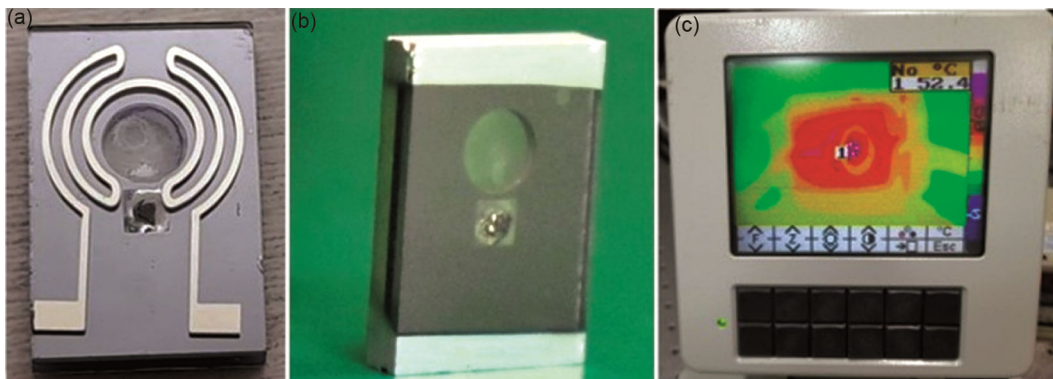


Fig. 2 — Heater integrated chip-scale Rb vapour cells (a) patterned NiCr heating element (b) ITO coated vapour cell with aluminum contact pads.(c) thermal image of the integrated chip-scale heater under test.

with its cap, holding all the internal components firmly in place. The positions and dimensions of the slots ensure optical alignment with a precision of about 0.1 mm of the optical head. This level of precision is adequate for obtaining a strong signal on the photodiode. The electrical leads of the photodiode, thermistor, and cell heaters are routed and terminated at another set of berg pin sockets. Finally a top cover is screwed on to the package holding the entire MO optic assembly together. All the parts of the MO package were designed using a CAD software package and produced in 3D printing tool using PLA material.

Photographs of the fabricated magneto-optic package and the showing placement of the internal components prior to assembly of the top cap and after assembly into the external housing with VCSEL and collimating lens are shown in Figs. 3 (a) and (b) respectively. The amplifier IC was mounted on an SMD chip carrier and housed in a compact 3D printed housing. The schematic of the I to V amplifier and the photograph of the fully

assembled MO package alongside the amplifier are given in Fig. 4.

The MO package was placed on a vibration isolated bench for optical testing. The output of the amplifier was branched into two, one branch was connected to an oscilloscope while the other was fed to the analog input channel of the DAQ. The DAQ was interfaced to a PC via USB. The precision current source for driving the VCSEL was interfaced to the PC via a GPIB interface. The temperature of the VCSEL was monitored by measuring the resistance of the integrated thermistor in the package. The temperature controller converts the set point and the process temperature to a voltages that were digitized by an arduino board (UNO) that was under the control of a Raspberry Pi single board computer (Model 3B). A programme in the Raspberry Pi was written to log and plot the set and process values of the VCSEL temperature with an update interval of 1 second. The laser temperature was set at 54 °C using

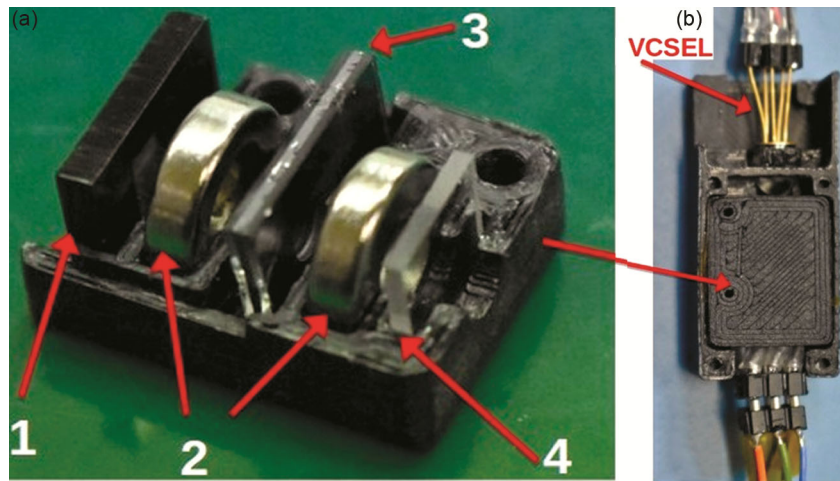


Fig. 3 — (a) showing the various components of the slotted MO housing 1-photodetector on an acrylic holder, 2-annular magnets, 3-heater integrated Rb vapour chip, 4- ND filter. (b) the closed slotted housing placed inside the outer housing.

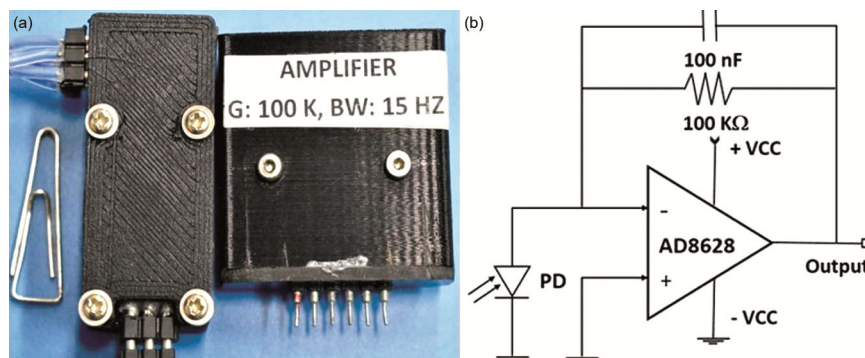


Fig. 4 — (a) Photograph of the fully assembled MO package and amplifier. (b) Schematic of the trans impedance amplifier circuit.

this system. The chip-scale cell heater in the package was heated to ≈ 75 °C by applying 3.5 V across it using a bench top power supply. About 700 mW to 800 mW power was dissipated by the ITO film vapour cell integrated heater. The system was left for about 10 minutes to attain thermal equilibrium. The current scan was initiated as per the set parameters using the graphical user interface (GUI) of the data acquisition software. Raw data consisting of the absorption peaks on a slanted baseline was observed on the oscilloscope as shown in Fig. 5 The oscilloscope is set to "roll mode" for continuous trigger free monitoring of the photodetector output.

If the entire spectrum is not seen in a single scan, the temperature of the VCSEL is adjusted such that the full spectrum is seen in the center of the scan. Subsequent to obtaining the complete spectrum on the oscilloscope data acquisition and analysis process is initiated using the "acquire" function of the GUI. The layout of the test set up is illustrated in Fig. 6.



Fig. 5 — Unprocessed absorption spectrum from chip-scale vapour cell observed on oscilloscope.

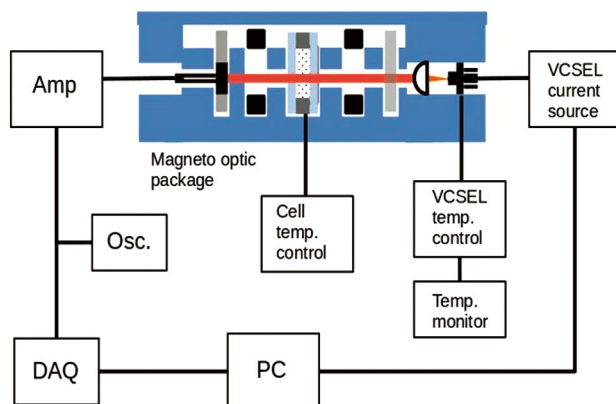


Fig. 6 — Layout of the experimental set up of the absorption spectroscopy of chip-scale Rb vapour cell.

4 Data Acquisition and Analysis

In this section, the details and features of the in-house developed data acquisition and analysis software for real time processing of the recorded spectral data are described. The output of the photo detector inside the magneto optical head is digitized by a compact data acquisition module (National Instruments USB-6009). The sampling rate is selected to be 5000 samples/s. The data from the DAQ is acquired in asynchronous mode as the VCSEL current is scanned across the D1 absorption lines of Rb atoms. The scanning was done using a sawtooth shaped laser current ramping up with time. Data captured over an acquisition time of 10 seconds is saved in the PC for further processing. The data processing software is implemented in MATLAB in the form of a user friendly GUI. The programme also allows the user to set the parameters of the current scan such as current range, step size and dwell time. The acquired data is automatically processed after the fixed acquisition time of 10 seconds. Since the acquisition is done in asynchronous mode, the acquired data has multiple sets of spectral data. In some instances, there may also be partial spectra. The program scans the acquired data and automatically isolates a single, complete spectral scan. This data is subjected to a box car averaging process to smoothen out experimental noise. The size of the averaging bin is carefully selected such that the noise is reduced and at the same time there is minimal loss of spectral information from the data set. The bin size used in this work was 200 points. Due to the nature of the VCSEL source, when the current is swept, not only the output frequency but also intensity changes. The VCSEL has a positive current tuning coefficient as mentioned in section 2.2. This results in the raw spectrum appearing on a slope. The next step is to remove this slope and get a flat baseline for the absorption spectrum. The captured data set is resized such that there are 2500 points on either side of the spectrum. Baseline slope is computed by fitting a straight line to the base line points on either side of the spectrum. The straight line fit is achieved using the POLYFIT function of MATLAB. The computed baseline is subtracted from the raw spectrum to get the absorption spectrum with a flat background (baseline). This is followed by the next processing step to locate the minima in the data set and identify the corresponding index numbers. The ISOLocal-MIN function of MATLAB is used to identify the minima. After this process, all minima in the dataset get

identified. To distinguish between the minima due to local fluctuations and those resulting from atomic absorption, a peak detection threshold value of 1 mV from the baseline is used. The next step is to generate the wavelength axis. In the raw data, the x-axis is index number. Since the nature of the Rb absorption spectrum is known, two peaks from the recorded data are considered as reference. The reference peaks correspond to the Doppler broadened lines $^{85}\text{Rb } F=2 \rightarrow F' = 2,3$ (794.985 nm) and $^{87}\text{Rb } F=1 \rightarrow F' = 1,2$ (794.980 nm)¹⁵. The wavelength step is computed by finding the difference in the reference peaks and deciding by the number of index points between them. After computing the wavelength step, the wavelength axis is produced by adding and subtracting the step value from any one of the reference peaks. In a similar fashion, a frequency axis can also be produced by converting the reference wavelength to frequency units. The parameters of absorption lines can be estimated by fitting Gaussian functions to them. The fitting was carried out for $^{85}\text{Rb}(^2\text{S}_{1/2} F=2 \rightarrow ^2\text{P}_{1/2} F' = 2,3)$ and $^{87}\text{Rb}(^2\text{S}_{1/2} F=2 \rightarrow ^2\text{P}_{1/2} F' = 1,2)$. For convenience, the identified absorption resonance peaks are numbered as given in Table 1. A typical screenshot of the GUI after acquiring the spectrum is given in Fig. 7.

5 Results and Discussions

Absorption spectroscopy studies of the chip-scale Rb atomic vapour cell have been carried out in a compact MO package. The Rb vapour is interrogated for the D1 absorption line of both ^{85}Rb and ^{87}Rb . The absorption spectrum is obtained by scanning the injection current of a VCSEL diode laser whose temperature is maintained to cover the wavelength window of interest.

The absorption spectrum of this hot atomic vapour in 3.5 μl volume has been recorded and analyzed. The acquired data is processed in real time and absorption spectrum with identified peaks along with FWHM based on Gaussian fitting of selected peaks are displayed at the click of a mouse button. Steady repeatable spectra have been obtained from the MO package for more than 600 hours of cumulative operation in lab conditions. These operations involve about 500 ON/OFF cycles. The repeatability of the results indicated the excellent mechanical and thermal stability achieved in this package. The obtained spectral parameters for two selected atomic resonance transitions are given in Table 2. The measurement uncertainties are obtained from standard deviation of 20 independent measurements of the parameter.

Absorption amplitude is defined as the value of the minimum detector output for the relevant transition. Its value depends on parameters such as characteristics of the detector and amplifier gain. The ratio of the detector output to the off resonance background expressed as a percentage is given in the brackets in

Table 1 — Labeling of absorption resonance peaks.

Peak	Transition
1	$^{87}\text{Rb}(^2\text{S}_{1/2} F=1 \rightarrow ^2\text{P}_{1/2} F' = 1, 2)$
2	$^{85}\text{Rb}(^2\text{S}_{1/2} F=2 \rightarrow ^2\text{P}_{1/2} F' = 2, 3)$
3	$^{85}\text{Rb}(^2\text{S}_{1/2} F=3 \rightarrow ^2\text{P}_{1/2} F' = 2, 3)$
4	$^{87}\text{Rb}(^2\text{S}_{1/2} F=2 \rightarrow ^2\text{P}_{1/2} F' = 1, 2)$

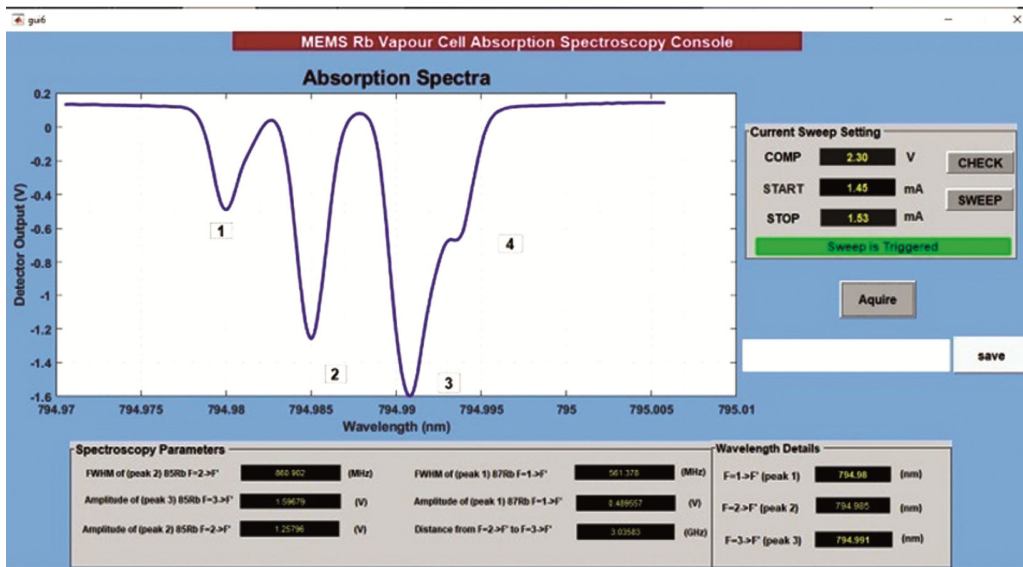


Fig. 7 —Screenshot of the GUI developed for acquiring and analyzing the absorption resonance spectrum of the chip-scale vapour cell in the MO package.

Table 2 — Spectral characteristics of selected absorption resonances chip-scale vapour cell obtained from the compact package at cell temperature of 70 °C.

Peak	Wavelength (nm)	FWHM (MHz)	Abs. amplitude (V)	Abs. Coefficient (m ⁻¹)
Peak 1	794.980	567±16	0.477±0.014 (19.08%)	433.42
Peak 2	794.985	850±15	1.24±0.017 (49.6%)	1370.36
Separation between Peak 2 and Peak 3			3.03583 GHz	

Table 2. This indicative of the strength of absorption in the atomic vapour medium.

The absorption coefficient, $\alpha(\lambda)$ can be calculated from the Beer-Lambert law $\alpha(\lambda) = \frac{-1}{d} \ln \left(\frac{I_o - I(\lambda)}{I_o} \right)$

Where d is the optical path length (500 μm), $I(\lambda)$ is the detector output at minimum intensity and I_o is the off resonance detector output. The argument of the natural logarithm represents the fraction of the incident light absorbed at the wavelength λ . In this system, the off resonance detector output was measured to be 2.5 V.

The results presented in Table 2 are for two typical absorption resonances in the chip-scale cell. At the cell temperature of 70 °C, the dominant line broadening mechanism is expected to be Doppler broadening due to thermal motion of atoms. It is known that Doppler broadening of the spectral lines is about 500 MHz. The measured line widths are higher than this value. This is due to the merging of the narrowly separated excited hyperfine states. For ⁸⁵Rb, the excited hyperfine states of the D1 line, 5P_{1/2} F=2 and F=3 states are separated by only 361 MHz, which is less than the Doppler broadening. These two resonances get merged resulting in a single broadened peak that is measured in the experiment. For ⁸⁷Rb, the excited state hyperfine states are separated slightly more than the Doppler line width viz., 814 MHz. In principle they should be resolvable in the spectrum. However due to the strong and broad absorption peaks of ⁸⁵Rb in the close vicinity, ⁸⁷Rb peaks get merged with the ⁸⁵Rb peaks. Instability in laser injection current and laser temperature also contribute to the broadening of absorption resonance lines, these factors have not been quantified in the present work. The frequency interval between peaks 2 and 3 is found to be 3.05 GHz, which agrees well with the literature values for the ⁸⁵Rb ground state hyperfine

levels^{15,16}. This separation is the so called clock frequency because of the important role it plays in timing applications.

6 Conclusions

In this work we have reported absorption spectroscopic studies on heater integrated chip-scale Rb vapour cells housed in a compact 3D printed MO package. A thermally stabilized, tunable VCSEL was used to interrogate the D1 resonance absorption lines of a natural mixture of ⁸⁵Rb and ⁸⁷Rb. Stable and repeatable spectra have been obtained from this package for over 600 cumulative hours of operation. Obtaining stable absorption spectrum is one of the primary requirements for developing atomic sensors using chip-scale vapour cells. The architecture of the MO package demonstrated in this paper is being augmented to function as a compact laser frequency stabilization system by incorporating quarter wave plate, polarizing beam splitter and balanced photodetector, which will find wide applications in space borne sensors and payloads.

Acknowledgements

The authors are thankful Sri M. Sankaran, Director, U R Rao Satellite Center for his keen interest and encouragement for carrying out this research work at LEOS.

References

- 1 Taylor M C D, Mouloudakis K, Zetter R, Hunter D, Lucivero V G, Bodenstedt S, Parkkonen L & Mitchell M W, *Phys Rev Appl*, 18 (2022) 14.
- 2 Sander T H, Preusser J, Mhaskar R, Kitching J, Trahms L & Knappe S, *Biomed Opt Express*, 3 (2012) 981.
- 3 R M Noor & Shkel A M, *J Microelectromech Syst*, 27 (2018) 1148.
- 4 Pustelny S, Schultze V, Scholtes T & Budker D, *Rev Sci Instrum*, 87 (2016) 107.
- 5 Dyer S, Gallacher K, Hawley U, Bregazzi A, Griffin P F, Arnold A S, Paul D J, Riis E & McGilligan J P, *arXiv*, (2022).
- 6 Haesler J, Balet L, Porchet J A, Overstolz T, Pierer J, James R J, Grossmann S, Ruffieux D & Lecomte S, *Joint European Frequency and Time Forum International Frequency Control Symposium, EFTF/IFC*, (2013) 579.
- 7 Park J, Hong H G, Kwon T Y & Lee J K, *IEEE Sens J* 21 (2021) 6839.
- 8 Holloway C, Simons M, Haddab A H, Gordon J A, Anderson D A, Raithel G & Voran S, *IEEE Antennas Propag Mag*, 63 (2021) 63.
- 9 Downes L A, MacKellar A R, Whiting D J, Bourgenot C, Adams C S & Weatherill K J, *Phys Rev X*, 10 (2020) 011.
- 10 Knappe S, *Comprehens Microsyst*, 3 (2007) 571.

- 11 Hasegawa M, Chutani R, Gorecki C, Boudot R, Dziuban P, Giordano V, Clatot S & Mauri L, *Sens Actuators A: Phys*, 167 (2011) 594.
- 12 Chutani R, Maurice V, Passilly N, Gorecki C, Boudot R, Hafiz M A, Abb'e P, Galliou S, Rauch J Y & Clercq E de, *Scient Rep*, 5 (2015) 14.
- 13 Ji Y, Shang J, Gan Q, Wu L & Wong C P, *IEEE Trans Comp Packag Manuf Technol*, 8 (2018) 1715.
- 14 Giridhar M S, Nandakishor M M, Dahake A, Tiwari P, Jambhalikar A, John J & Karanth S P, *ISSS J Micro Smart Syst*, 11 (2022) 427.
- 15 Nishino H, Hara M, Yano Y, Toda M, Kanamori Y, Kajita M, Ido T & Ono T, *Appl Phys Exp*, 12 (2019) 072.
- 16 Ben-Aroya I & Eisenstein G, *Proc IEEE Int Freque Control Sympos Exposit*, 2005 (2005) 602.